Science Advances

AAAS

advances.sciencemag.org/cgi/content/full/2/1/e1501104/DC1

Supplementary Materials for

Tunable light emission by exciplex state formation between hybrid halide perovskite and core/shell quantum dots: Implications in advanced LEDs and photovoltaics

Rafael S. Sanchez, Mauricio Solis de la Fuente, Isaac Suarez, Guillermo Muñoz-Matutano, Juan P. Martinez-Pastor, Ivan Mora-Sero

Published 22 January 2016, *Sci. Adv.* **2**, e1501104 (2016)
DOI: 10.1126/sciadv.1501104

The PDF file includes:

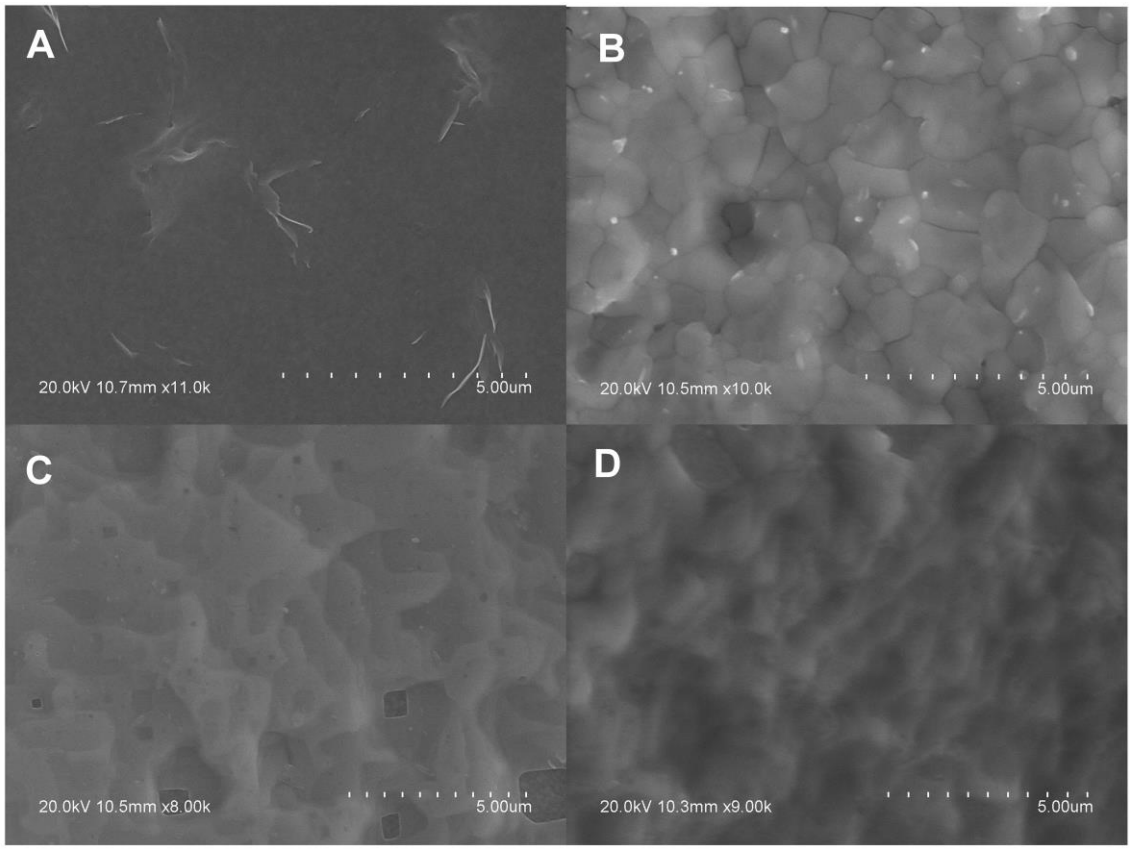

Figure S1: SEM picture of the surfaces of (**A**) compact TiO_2, (**B**) QD 3 nm, (**C**) perovskite, (**D**) PS/ QD 3 nm and (**E**) QD/PS 3 nm layers.

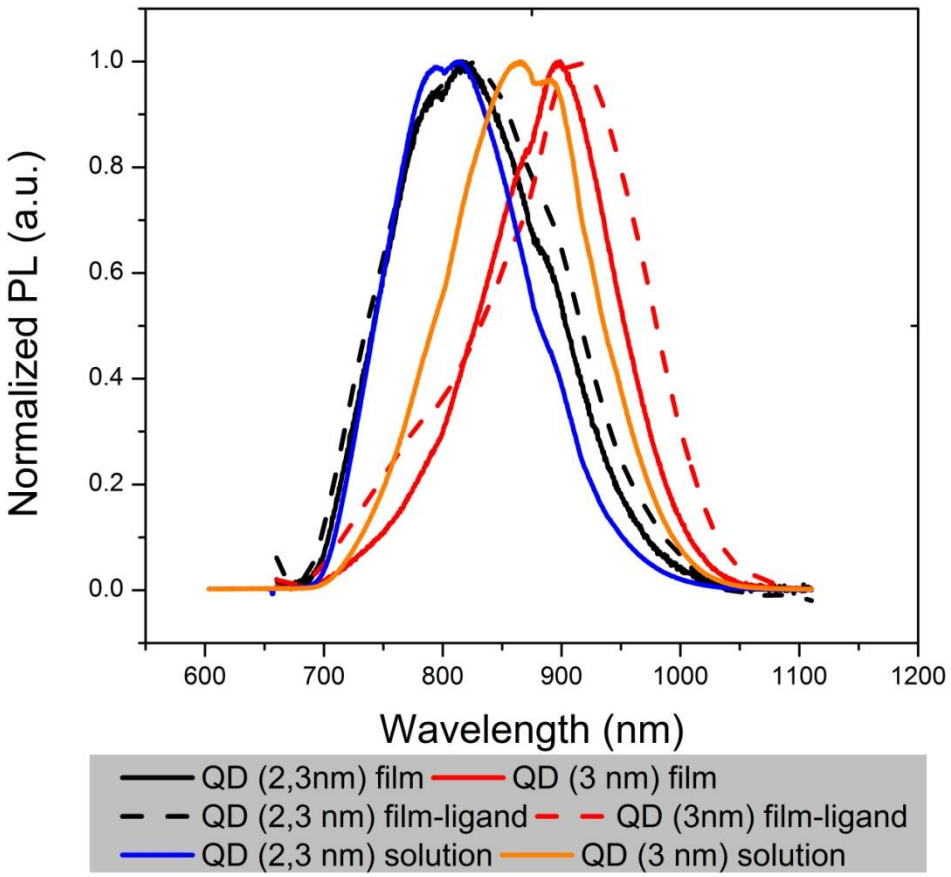

Figure S2: Normalized PL for both kind of QDs prepared in this work. PL from QD solution is compared with the PL obtained from the film after QD deposition by spin coating and with the PL obtained for the same layer after ligand exchange in order to obtain a MPA capping. Note the successive red shifts produced first after film deposition and after ligand exchange. Each one of the processes brings QDs closer from the other relaxing the quantum confinement.

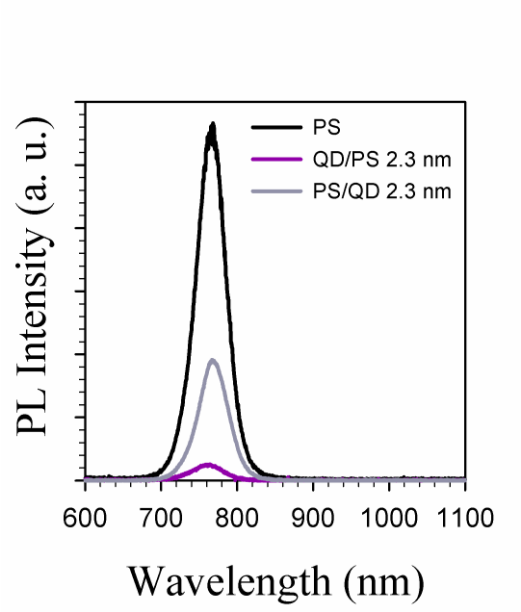

Figure S3: PL of PS single layer and from bilayers, QD/PS and PS/QD, using 2.3 nm QDs.

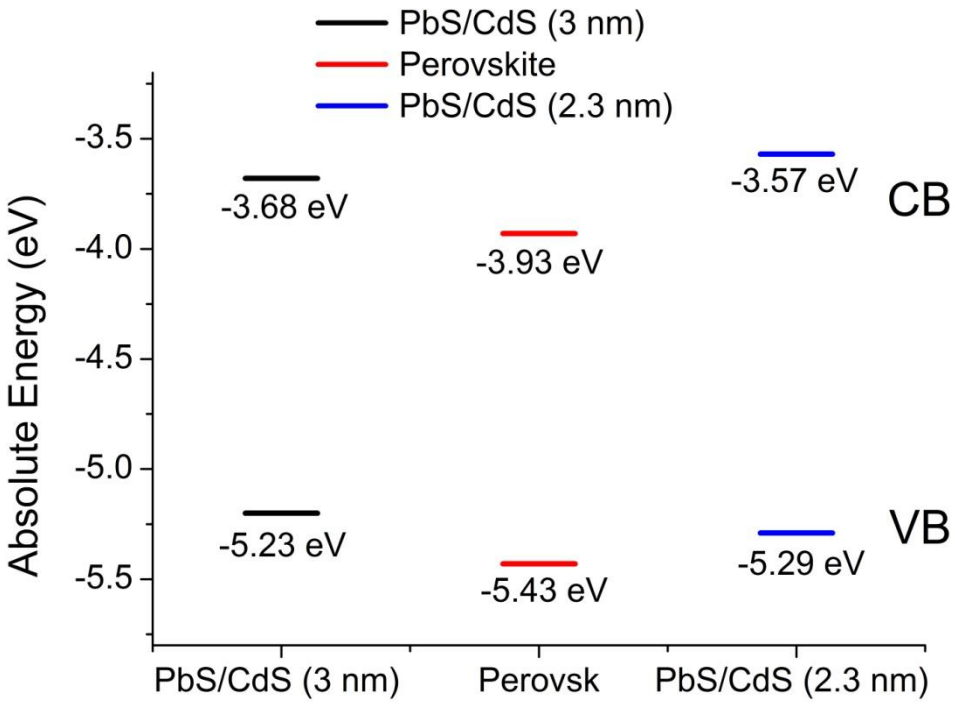

Figure S4: Conduction Band (CB) and Valence Band (VB) of perovskite extracted from Ref. (*4*). Values for CB of PbS QDs have linearly extrapolated from values reported in Ref. (*22*). The results are also in good agreement with the values measured for PbS QDs with MPA capping reported in Ref. (*23*). Values for VB of PbS have been obtained subtracting the QD band gap. This values have to be taken just as a rough estimation as CdS shell or possible surface or interface dipoles are not taken into account.

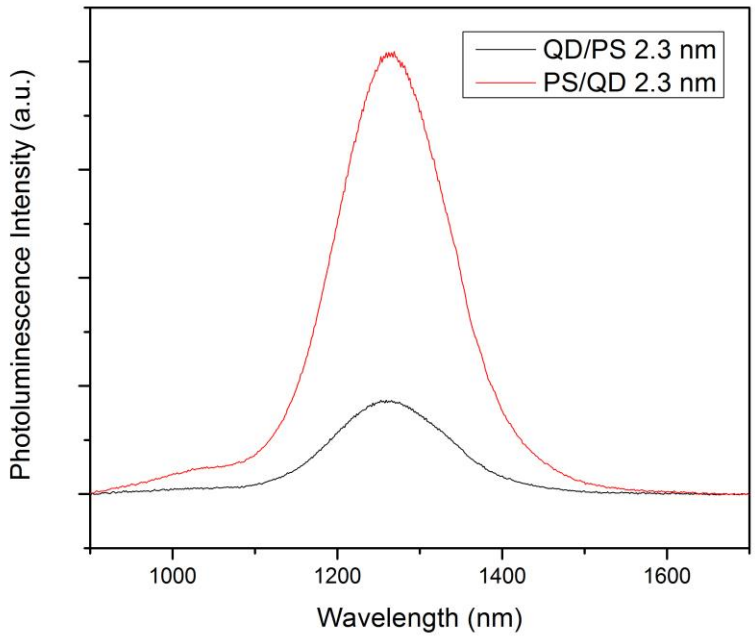

Figure S5: Comparison of the exciplex PL for QD/PS and PS/QD samples with QDs 2.3 nm.

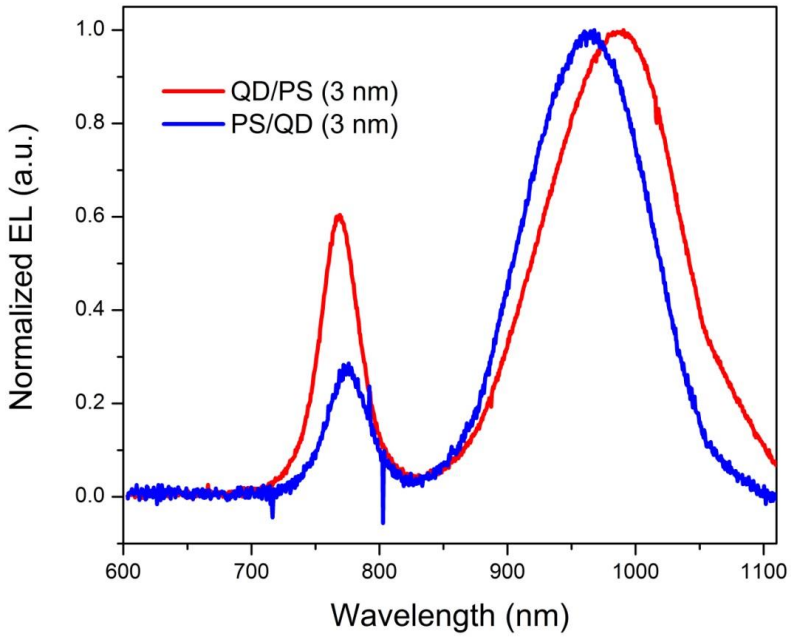

Figure S6: Normalized electroluminescence at V_{app} = 2V for bilayers fabricated with 3 nm PbS/CdS core/shell QDs. A red shift of the peak corresponding to the QD is observed for QD/PS sample in comparison to PS/QD. This shift could be attributed to the penetration of perovskite into the pores of the QD layer with the subsequent decrease of the quantum confinement.

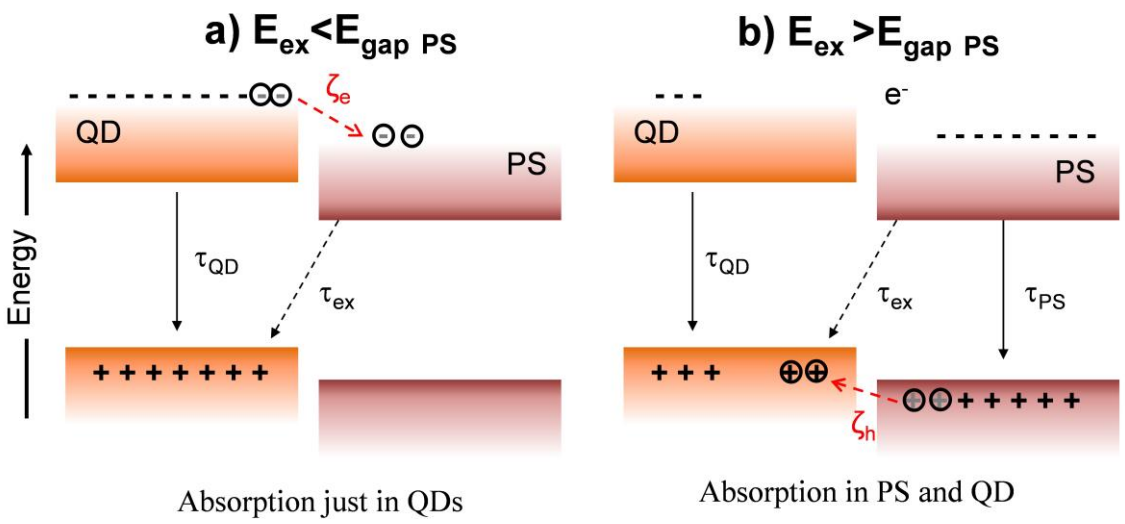

Figure S7: The exciplex state is formed by an indirect transition from the conduction band of the PS and the valence band of the QD. Then, if we excite with photons of energy, E_{exc}, below the PS absorption band-edge, $E_{gap\ PS}$ (scheme **a)** the carriers are only photogenerated at the QD layer (N1 photogenerated electron-hole pairs), but electrons can partially be transferred to the PS conduction band, with a transfer time ζ_e, and hence we would observe two PL bands, one of the QD direct transition and that of the exciplex (with characteristic decay times τ_{QD} and τ_{ex}, respectively; obtained from transient PL measurements, Fig. 2F). For excitation energies above the absorption band-edge of the PS (scheme **b),** carriers will be mainly photogenerated at the PS due to the large absorption coefficient and thickness (but also a certain portion are being photogenerated at the QD layer, approximately the same quantity N1 that were photogenerated under below bandgap excitation). In this case, holes can be partially transferred, with a transfer time ζ_h, towards the valence band states of the QDs (see scheme **b**). In this case we will observe three PL signals: PS (PL decay time τ_{PS}), QDs and exciplex, but exciplex intensity is one order of magnitude larger than that observed for below bandgap excitation (i.e. the ratio between integrated PL at excitation wavelength 740 nm and integrated PL at excitation wavelength 810 nm is ~10, see Fig. 2E). This fact is telling us that exciplex increases in the same quantity, well above N1 (giving the non-zero intensity of the PL signal for wavelengths longer than 800 nm). Furthermore, this enhancement of the exciplex signal when excitation is done above the PS bandgap is giving us an estimate of the transfer efficiency, determined by the ratio of hole transfer time over the PS decay time, (τ_h/τ_{PS}); therefore considering that this time ratio is similar to the ratio between the integrated PL and that $\tau_{PS} \approx 1$ ns, as it has been obtained from transient PL measurements, Fig. 2F, the hole transfer time would be of the order of 100 ps.

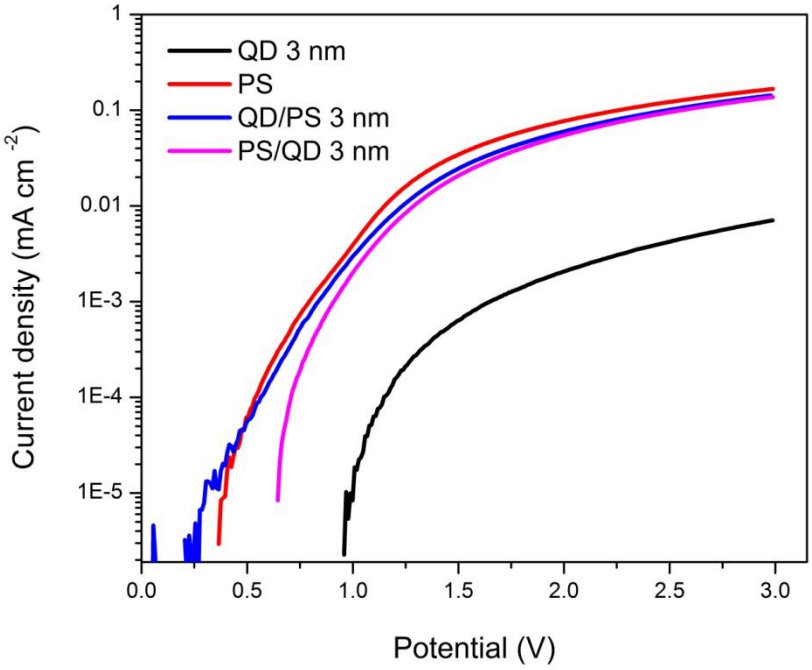

Figure S8: Current Potential (J-V) curve of the prepared LEDs. Similar curves are observed for PS and QD/PS bilayer pointing to a control of the transport properties by the PS. Much lower current have been recorded for QD LEDs indicating a higher resistivity.

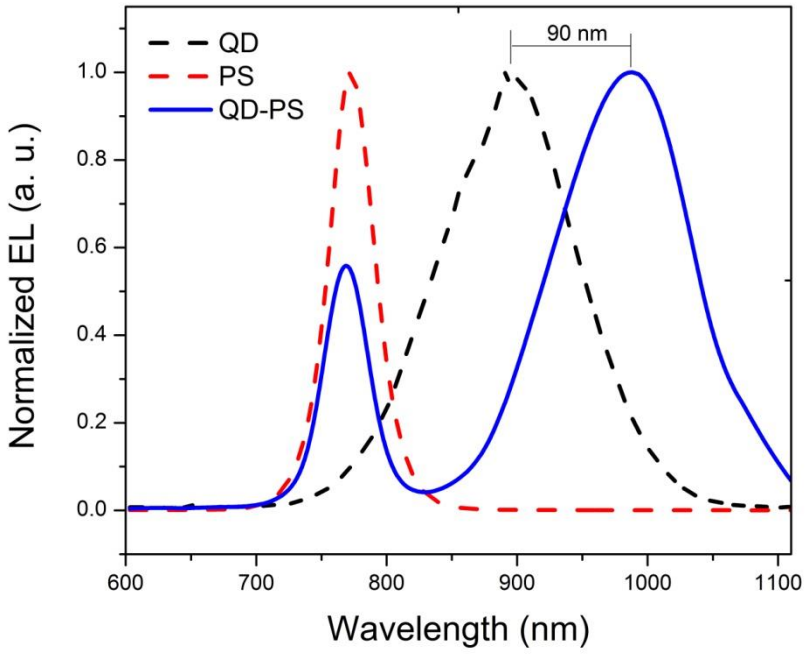

Figure S9: Normalized electroluminescence at V_{app} = 2V obtained from single layer LEDs prepared with PS and QDs and for a QD/PS (3 nm) bilayer. The peak corresponding to the PS emission is slightly blue shifted while QD peak has a strong red shift of 90 nm. This shift is less pronounced for PS/QD configuration, see fig. S4.

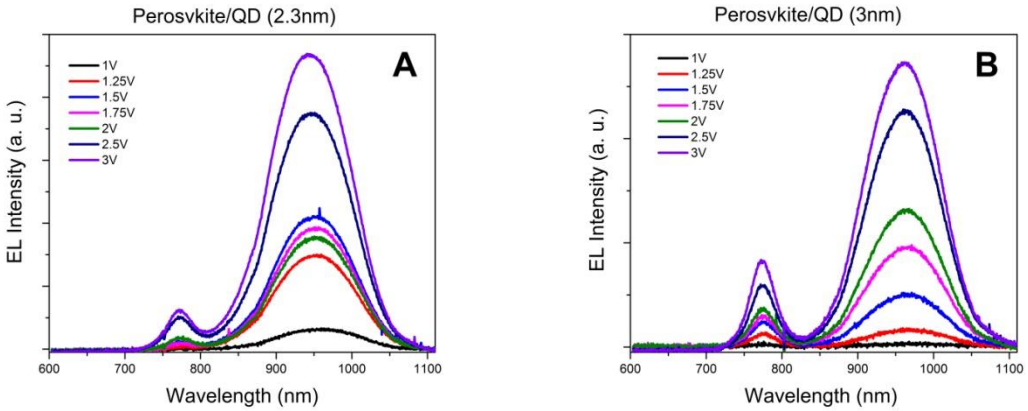

Figure S10: Electroluminescence at different V_{app} of PS/QD LEDs with (**A**) 2.3 nm QDs and (**B**) 3 nm QDs.

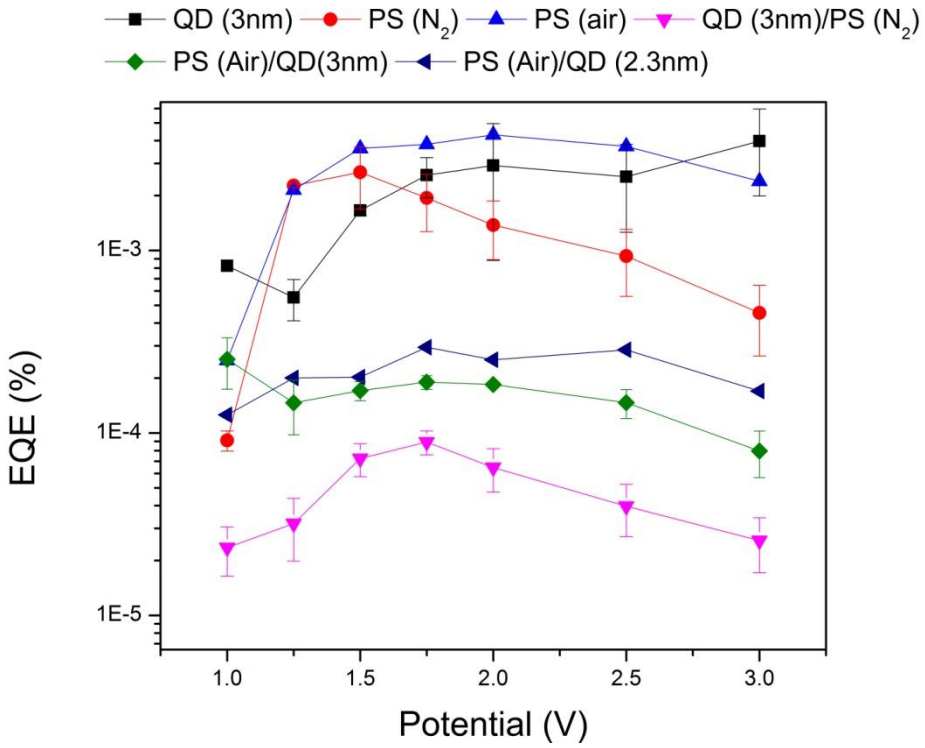

Figure S11: Average External Quantum Efficiency (EQE) at different V_{app} for different LEDs, including single layer (QD and PS annealed under air and N_2 atmosphere) and bilayers QD/PS and PS/QD. Average values and error bars have been obtained after measuring 4-6 LEDs prepared at each conditions. When perovskite is annealed (see materials and methods section) under N_2 atmosphere lower performance is obtained. Values obtained for bilayers are underestimated as just emission in the wavelength range from 600 to 1100 nm has been analyzed, and consequently emission from exciplex state is excluded because the analysis of both wavelengths ranges represents a technical limitation of our equipment, since two different photodetectors integrated in

the same calibrated system are required for the quantitative measurements in both wavelength ranges.